Analysis of Rainfall-Induced Shallow Slope Failure

Tehseena Ali[1], Himanshu Rana[2] and G.L. Sivakumar Babu[3]

[1]IISc Bangalore, Bengaluru 560012, India
[2]IISc Bangalore, Bengaluru 560012, India
[3]IISc Bangalore, Bengaluru 560012, India
tehseena.ali0578@gmail.com

Abstract. Rainfall-induced shallow slope failure has proved to be disastrous in many parts of the world. Majority of slope failures pose a significant risk to infrastructure and public-safety largely due to rainfall-induced slope failures. The stability analysis of slope generally seeks to understand the cause of the slope failure. The penetrating water reduces matric suction within the soil thereby reducing the shear strength of the soil slopes. In this direction, this paper attempted to analyze the slope behavior under different rainfall intensities and at slope angles. A series of numerical analysis was conducted under a fully coupled flow-deformation in PLAXIS finite-element modeling code. The numerical trials to check the stability of slope were performed under two dissimilar states, (1) rainfall of certain intensity was applied to the slope for a period of 24 hours, and (2) the slope stability was analyzed using soil nailing technique. Different rainfall intensities were applied to evaluate the maximum deformation and variation of pore-water pressure of the shallow slope. Results showed that with increasing rainfall duration, slope deformation increased thereby making the slope unstable. In addition, it is observed that the horizontal deformation in case of the reinforced slope gets reduced, hence increasing slope stability.

Keywords: Rainfall-induced slope failure, PLAXIS, Coupled flow, Soil nailing, Grouted nails.

1 Introduction

Kashmir often experiences precipitation-triggered landslides on national highway NH-44, which is the lifeline of Kashmir valley as well as Leh-Ladakh area. These landslides result in the closure of the highway for the most part of the year, thus considerably affecting the normal life of people. At soil-atmosphere interface, the flux boundary conditions (i.e., infiltration and evaporation) directly affects the characteristics of major parameters of slope stability like matric suction, the flow of water and strength of the soil. The rise of water pressure and groundwater level and reduction in matric suction during rainy seasons results in more frequent slope failures. Cai &Ugai [1] concluded that hydraulic characteristics of soil, initial volumetric moisture content, the intensity of rainfall and duration of rainfall significantly affect the water pressure in slopes which in turn results in instability of slope during rainfall. It was

deduced from the analysis done by Zhang et al. [2] that rainfall intensity was the main parameter influencing the matric suction under steady-state conditions, whereas in case of transient flow conditions, water storage function and saturated permeability along with rainfall infiltration affect the profile of matric suction. An analytical formulation was used by Collins et al. [3] which verified that positive pore-water pressure gets developed during high infiltration rates in coarse-grained soils and therefore seepage forces lead to the failure in the slope. Whereas, in the case of fine-grained soils with low infiltration rates, loss of suction occurs which leads to a reduction in shear strength and thus the failure of slope.

Understanding the precipitation-initiated slope failure problem requires mechanical modeling and flow simulation, particularly in an unsaturated groundwater flow condition. A common theory related to groundwater flow and mechanical deformation was previously embraced for different numerical examinations. In such theories, as presented by Rahimi et al. [4], the flow field of groundwater was decoupled from the field of mechanical deformation. However, the interaction between the hydraulic field and mechanical field is the basic reason of rainfall-induced slope failures and thus a strong tool is required to coordinate a progression of numerical trials for the study of such problems. These problems can be more precisely simulated by coupling the hydrological-mechanical behavior as done by Chinkulkijniwat et al. [5]. A series of parametric studies were performed by Yubonchit et al. [6] and the results demonstrated that slope failure may occur during infiltration stage or rising water table stage and depends on the infiltration capacity at saturated state. At saturated state, if infiltration capacity is higher than rainfall intensity, the slope is steady due to residual matric suction throughout the infiltration stage and may fail during rising water table stage. Whereas, if rainfall intensity exceeds the infiltration capacity at the saturated state, matric suction completely vanishes throughout the infiltration stage, and consequently more chances of the slope failure during the infiltration stage.

Among several slope stabilization techniques, soil nailing is an economical and straightforward remedial measure. The soil slopes that are unstable in nature are being treated by soil nailing; existing slopes are particularly being reinforced using this technique. The essential idea of soil nailing includes raising shear strength of the in-situ soil and restricting its deformation by placing reinforcing components which are moderately slender and are spaced close to each other, thereby creating a rational gravity structure. Limit equilibrium method (LEM) and several working stress design methods are among the different soil nailing design methods. The tensile forces that are resisting in nature get developed in the inclusions and are passed on through friction mobilized at the soil/nail interfaces into the soil thereby; restricting the deformation of soil and limiting failure during excavation as discussed by Luo et al. [7]. Yuan et al. and Babu & Singh [8, 9] draw a conclusion that soil and nail parameters are vulnerable in nature as a result of which there are still the chances of failure, therefore, in order to assess the stability a helpful probability method should be proposed and applied.

The main objective of the current study is to examine the slope behavior under different rainfall intensities and to check the response of soil nails in case of the reinforced slope. The analysis was conducted with shallow slope (unreinforced and rein-

forced) under finite element conditions. A few numerical examinations were performed to analyze the maximum deformation, variation of pore-water pressure and development of axial forces in soil nails. In case of the nailed slope, axial force plays the main part in stabilizing the slope than bending and shear force therefore; only axial force is considered in the analysis.

2   Methodology

A finite-element modeling code PLAXIS [10], with fully coupled flow-deformation, was used here for the analysis. In association with the unsaturated conditions, shear strength of soil was stated using the Mohr-Coulomb failure criterion and bishop's effective stress concept as expressed in equation 1. In order to simulate transient flow through unsaturated soil, Richard's equation [11] was used as the hydrological process.

$$\tau = c' + (\sigma_n - u_a)tan\phi' + \mathcal{X}(u_a - u_w)tan\phi' \tag{1}$$

where τ = shear strength of unsaturated soil; $_n$= total normal stress; u_a and u_w are pore air pressure and pore-water pressure respectively; $(\sigma_n - u_a)$ = net normal stress; $(u_a - u_w)$ = matric suction; c' = effective cohesion; $'$ = internal soil friction angle; and $\mathcal{X}$ = scalar multiplier.

In the case of unsaturated zones, the permeability is depicted by the soil water characteristics curve (SWCCs). The relation between pressure head and moisture content is termed as SWC. Van Genuchten model and van Genuchten-Mualem model explain SWC, and the permeability function respectively. Equation (2) and (3) presents the van Genuchten model and van Genuchten-Mualem model are respectively:

$$\theta_e = \frac{\theta_w - \theta_{res}}{\theta_{sat} - \theta_{res}} = \left[\frac{1}{1 + \{\alpha(u_a - u_w)\}^n}\right]^{1-1/n} \tag{2}$$

$$k(h) = k_{sat}\frac{[1 - \{\alpha(u_a - u_w)\}^{n-1}[1 + \{\alpha(u_a - u_w)\}^n]^{1/n-1}]^2}{\{1 + \{\alpha(u_a - u_w)\}^n\}^{1/2 - n/2}} \tag{3}$$

Where $_w$, $_{res}$ and $_{sat}$ denotes volumetric moisture content, residual volumetric moisture content, and saturated volumetric moisture content respectively. Saturated permeability of soil is represented by k_{sat}, and   and n are the fitting parameters. The parameters required in PLAXIS to carry out an analysis for slopes exposed to rainfall infiltration include strength parameters (c',   ) and hydraulic-related parameters (a, n, k_{sat}).

In PLAXIS, a plane-strain condition was used to model the soil nails. In order to simulate soil nails, plate structural elements can be used as they account the bending stress [12]. To simulate the plate elements, flexural rigidity (bending stiffness) *EI* and the axial stiffness *EA* are main input parameters. For the proper simulation of circular soil nails as rectangular plates, equivalent axial and bending stiffness's are used. To consider, the role of elastic stiffness's of grout envelope and reinforcement bar, equivalent modulus of elasticity E_{eq} was used and was determined as:

$$E_{eq} = E_n \left(\frac{A_n}{A}\right) + E_g \left(\frac{A_g}{A}\right) \tag{4}$$

Where: E_g, E_n, and E_{eq} are elasticity modulus of grout material, elasticity modulus of a nail, and equivalent elasticity modulus of grouted soil nail respectively, A_n is the total cross-sectional area and A is the area of grout cover. Knowing horizontal spacing S_h, drill hole diameter D_{DH}, and the equivalent modulus of elasticity (equation 4), axial and bending stiffnesses were determined from equations (5) and (6) respectively.

$$Axial\ stiffness\ EA\ [kN/m] = \frac{E_{eq}}{S_h}\left(\frac{\pi D^2_{DH}}{4}\right) \tag{5}$$

$$Bendi\ \ stiffness\ EI\ [kN/m] = \frac{E_{eq}}{S_h}\left(\frac{\pi D^4_{DH}}{64}\right) \tag{6}$$

3 Materials and methods

Soil properties adopted in this study were gathered from the relevant literature on slope failure together with Yubonchit et al. [9]. An elastoplastic model was used for soil with yield criterion of Mohr-Coulomb and the hydraulic behavior was modeled as a van Ganuchten model. The soil parameters for Mohr-Coulomb comprising strength, hydraulic and deformation parameters are tabulated in Table 1..

Table 1. Soil Parameters adopted for Mohr-Coulomb Model

Material property	Parameter	Symbol	Value	Unit
Mechanical	Mechanical model	_	Mohr-Coulomb	
	Material type	_	Undrained A	
	Cohesion	c	7	kPa
	Friction angle		36	Degrees
	Modulus of elasticity	E	30,000	kPa
	Poisson's ratio		0.3	_
Hydraulic	Hydraulic model	_	Van Genuchten	_
	Saturated permeability	k_{sat}		m/s
			1.56	_
			0.16	kPa^{-1}
General	Dry unit weight	$unsat$	17	kN/m^3
	Total unit weight	sat	17	kN/m^3

Soil nails in reinforced slope were modeled as plate elements available in PLAXIS. 6 rows of soil nails were assigned as shown in **Fig. 2** and the length of each nail was 4 m. The vertical spacing for the bottom 4 rows was 2 m and for the top 2 rows was 3m. **Error! Reference source not found.** gives the parameters adopted for the simulation of soil nails.

Table 2. Parameters adopted for numerical simulations of soil nails

Parameter	Symbol	Value	Unit
Material model	–	Elastic	–
Nailing type	–	Grouted	–
Yield strength of reinforcement	f_y	415	MPa
Nail diameter	D	0.02	m
Drill hole diameter	D_{DH}	0.1	m
Length of nail	L	4	m
Declination w.r.t horizontal	I	15	degree
Modulus of elasticity of nail	E_n	200	GPa
Modulus of elasticity of grout	E_g	22	GPa

As plotted from equation 4, with the magnitudes from **Table 1.**, **Error! Reference source not found.** shows the soil-water characteristic curve (SWC). The parameters like c', $'$, , and , were kept constant with the value of 7 kPa, 36˚, 0.16 kPa-1, and 1.56 respectively. A saturated permeability of 1×10-5 m/s was used in the examination.
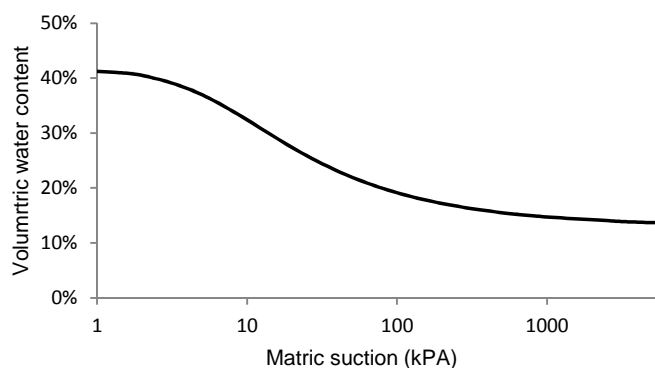
Fig. 1. SWC curve

The study was carried out on two different types of slopes, a) slope without any reinforcement, and b) slope reinforced with soil nails. Three different rainfall intensities viz., 24.8, 20 and 13.75 mm/hr were applied on the slopes to check the stability and deformation of the slope. The rainfall intensities were derived from the intensity-duration-frequency (IDF) relationship of Srinagar area of Jammu and Kashmir (J&K) with a return period of 1, 10 and 50 years [13]. The simulation consists of 12 cases of a simulation run, 6 cases for a slope with 60˚ and 70˚ each. A rainfall period of 24 hours was used in all 12 cases. Out of 12 cases, 6 cases were conducted on the unreinforced slope and other 6 on the reinforced slope and for each slope, aforementioned rainfall intensities were assigned.

4   Analysis Setup

A finite element model with two-dimensional plane-strain was arranged to represent a 15 m high slope with an inclination of 60 & 70˚ to the horizontal. Fifteen noded triangular finite-element mesh is used. Slope geometry, fixity and boundary conditions allotted for the study are shown in Fig. 2. A steady-state flow calculation was performed before assigning desired rainfall intensity. Initially, the pore-water pressure was supposed to vary from -100 kPa to 0 kPa from top of the slope to the bottom of slop, which represents the conditions of ground before the application of rainfall. At the bottom boundary, no lateral and vertical movements were allowed, whereas, the only vertical movement was allowed along the right and left boundary. The preferred intensity of rainfall was applied along the inclined surface CD as boundary flux. Boundaries AB, GH, and AH were defined as impervious boundaries, while, along the side boundaries BC and EF while, boundaries were no flux was assigned.
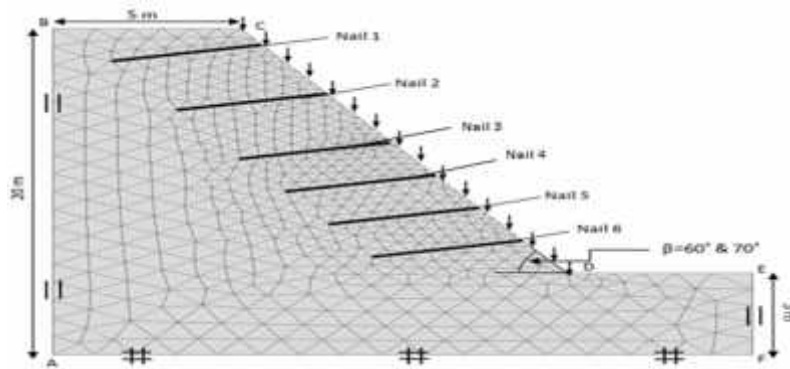
Fig. 2. Slope geometry and boundary conditions

After 2 to 3 days of drainage of surplus water, there is insignificant free drainage and the remaining water content held in the soil is termed as the water content at field capacity ($_{fc}$). For any soil type which has pore water pressure of -34 kPa corresponds to $_{fc}$ [14]. If no extra water is added for 2 to 3 days after precipitation, the moisture content may further diminish due to consumption by plant roots and evaporation. Therefore, the value of $_i$ is possibly between $_{fc}$ and $_{res}$. The pore water pressure allotted to the model ranging from -100 to 0 kPa presents the range of water content from 0-19% as per SWC of the model in **Error! Reference source not found.**.

5   Results and Discussion

Numerical investigation results are displayed and discussed as three perspectives: (1) maximum deformation attribute of slope exposed to specific precipitation, (2) the

probable failure mechanism identified with the response of pore-water pressure, and (3) variation of maximum axial forces of different nails with varying rainfall intensity.

5.1   Maximum deformation attribute of slope exposed to a specific precipitation
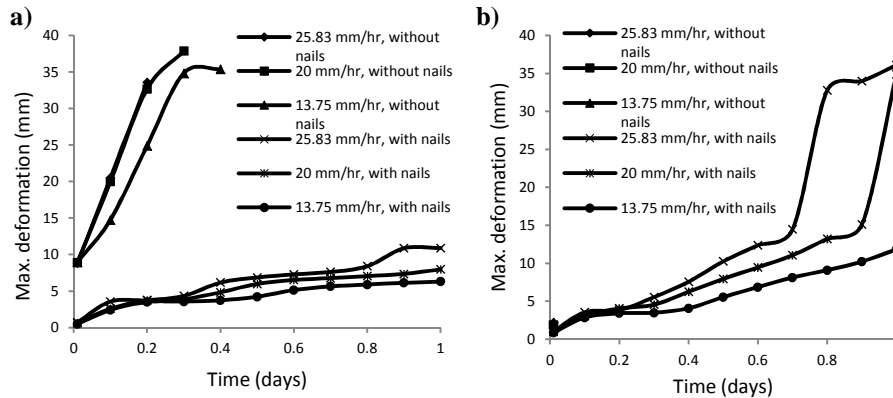
Fig. 3. Deformation attribute of slope (with and without soil nails) exposed to a constant rainfall intensity (a) slope angle 60°, and (b) slope angle 70°

The comparison of the maximum displacement of the slope with and without soil nail reinforcement against the simulated rainfall duration is demonstrated in **Error! Reference source not found.**. The figure presents the comparison for slopes with two different slope angles (= 60° and 70°) and for three rainfall intensities (25.83, 20, and 13.75 mm/hr). The unreinforced slope with a slope angle of 60° and rainfall intensities of 25.83, 20, and 13.75 mm/hr failed after 0.2, 0.3, and 0.4 days of rainfall infiltration. While, the soil nailed slope with same inclination (i.e., 60°) and rainfall intensities of 25.83, 20, and 13.75 mm/hr had maximum displacements of 10.89, 7.97, and 6.31 mm respectively after rainfall duration of 24 hours.

In case of the slope with 70° slope angle, the failure was observed only after 0.1 days of rainfall duration for all the three rainfall intensities. Whereas, the maximum displacements of the soil nailed slope with a slope angle of 70° were 36.1, 34.9, and 11.8 mm for rainfall intensities of 25.83, 20, and 13.75 mm/hr respectively and rainfall duration of 24 hours. The examination result demonstrated that the deformation of the slope was reduced significantly by the impact of soil nails. The displacement of the slope after the end of the rainfall was restricted as well.

5.2   The possible failure mechanism identified with the response of pore-water pressure:

To study the response of pore water pressure in the shallow layer, vertical sections of depth 3 meters were selected at the maximum deformation zone for analysis. The pore

water pressure profiles for slopes with slope angle 60° and 70° are shown in **Error! Reference source not found.** and **Error! Reference source not found.**. Two stages can describe the pore-water pressure: a stage of rainfall infiltration and a stage of water table rising. Throughout the infiltration stage, the magnitude of the negative pore-water pressure keeps decreasing from the initial value and achieves a single highest magnitude. Therefore, at any depth, the value of pore-water pressure is this single highest value. Hydraulic properties and flux boundary of the soil effects this constant value of pore water pressure [6]. At shallow depths, negative pore-water pressure starts to dissipate immediately after the initiation of rainfall.
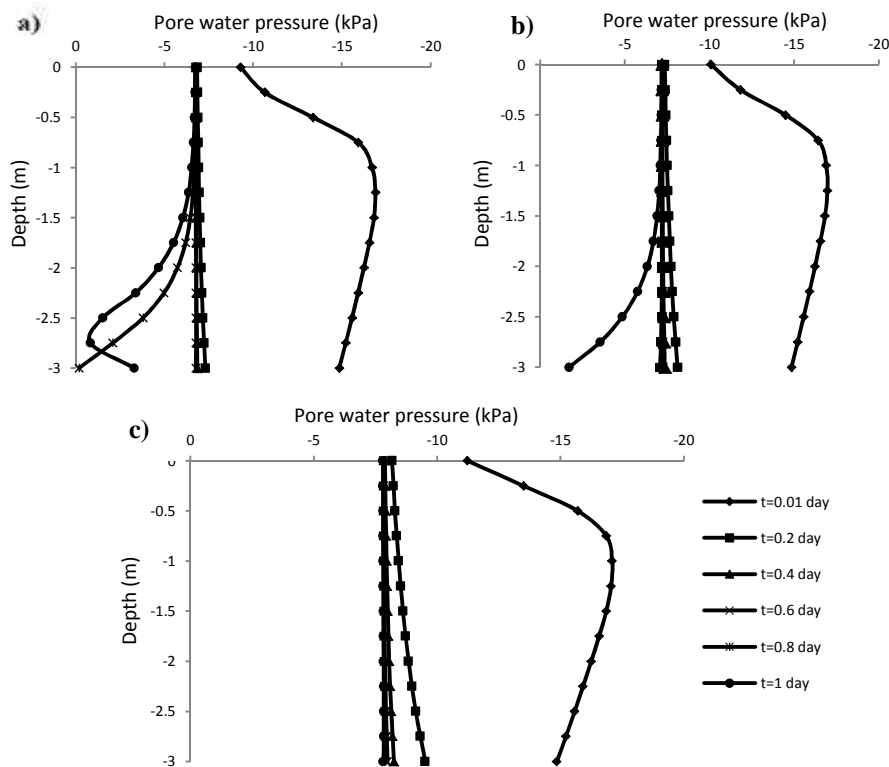
Fig. 4. Development of pore-water pressure profile for the reinforced slope with = 60° for different rainfall intensities a) $i = 25.83$ mm/hr, b) $i = 20$ mm/hr and c) $i = 13.75$ mm/hr

Error! Reference source not found. shows the pore water pressure profile of reinforced slope with slope angle 60° and rainfall intensities 25.83, 20, 13.75 mm/hr. For the rainfall intensity of 25.83 mm/hr pore-water pressure ranges from -6.7 kPa to -0.84 kPa, for rainfall intensity of 20 mm/hr, it ranges from -7.1 kPa to-1.8 kPa, and for rainfall intensity of 18.75 mm/hr it reaches to a value of -7.8 kPa with depth. Similarly, **Error! Reference source not found.** presents the change in pore water pressure for the reinforced slope with slope angle 70°. It is seen that for the rainfall intensity of 25.83 mm/hr ranges from -6.3 kPa, for rainfall intensity of 20 mm/hr, it ranges from -

6.7 kPa, and for rainfall intensity of 18.75 mm/hr it reaches to a value of -7.4 kPa with depth.

a)

Pore water pressure (kPa)

b)

Pore water pressure (kPa)

c)

Pore water pressure (kPa)
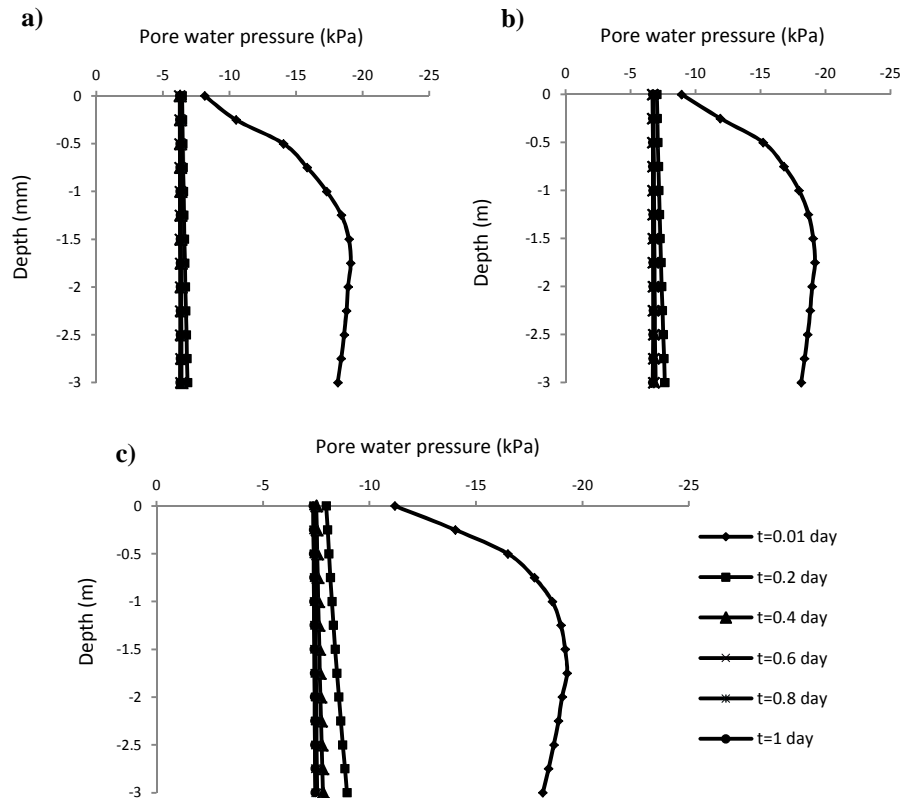
Fig. 5. Development of pore-water pressure profile for the reinforced slope with ϕ = 70° for different rainfall intensities a) i = 25.83 mm/hr, b) i = 20 mm/hr and c) i = 13.75 mm/hr

5.3   The variation of maximum axial force of different nails with varying rainfall intensity:

The development of axial forces in soil nails in case of the reinforced slope was analyzed for all nails at different positions were selected. Nail 1 and 2 were from the upper portion of the slope, nail 3 and 4 were from the middle portion of the slope, whereas, nail 3 and 4 were from the lower portion of the slope. **Fig. 6** and **Error! Reference source not found.**show the distribution of maximum axial force in nails for the duration of 24-h rainfall. The positive stress represents the tensile force and the negative stress represents compressive force. As shown in the figures, the maximum axial forces in the Nail 1 were approximate 0 for the slope with ϕ = 60° (**Fig. 6**) and became tensile for higher rainfall intensity for the slope with ϕ = 70° (**Error! Reference source not found.**). The maximum axial force in the remaining nails was tensile in nature for both the cases (i.e., ϕ = 60 & 70°) for all rainfall intensities. Axial force

for Nail 6 was largest for all the cases. In the case of the slope with $= 60°$, as depict-
ed in **Fig. 6** the axial forces are increasing at a very low rate and the highest value of
Nail 1 after 24 hours of rainfall reaches to 64.5, 56.4, and 53.4 kN/m for rainfall in-
tensities of 25.83, 20, and 18.75 mm/hr.

a)   b)

c)
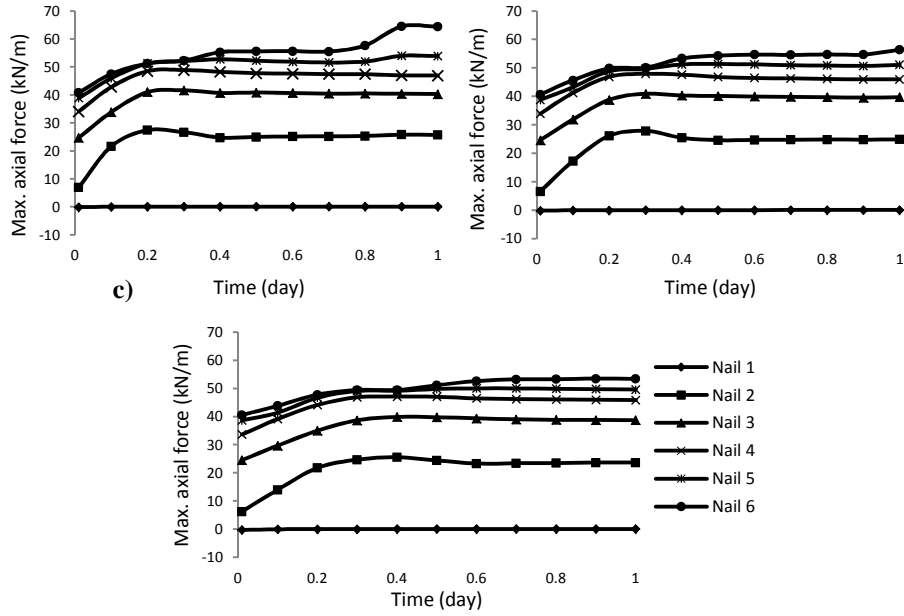
Fig. 6. Variation of axial forces for different nails at different time intervals for slope with $=$
60° a) $i = 25.83$ mm/hr, b) $i = 20$ mm/hr, and c) $i = 13.75$ mm/hr

a)   b)

c)
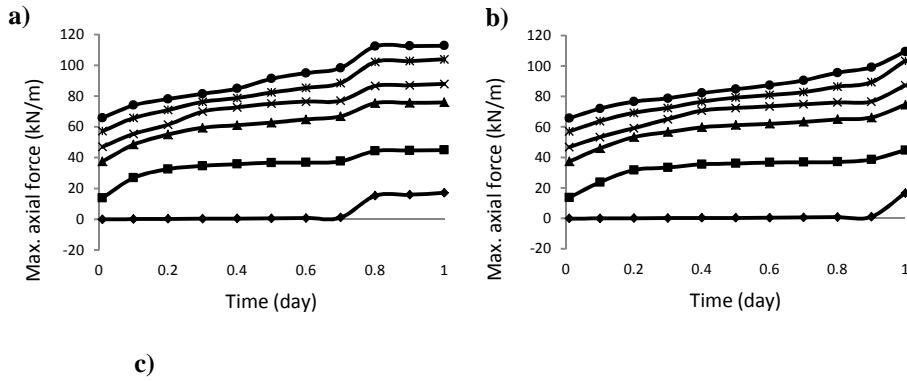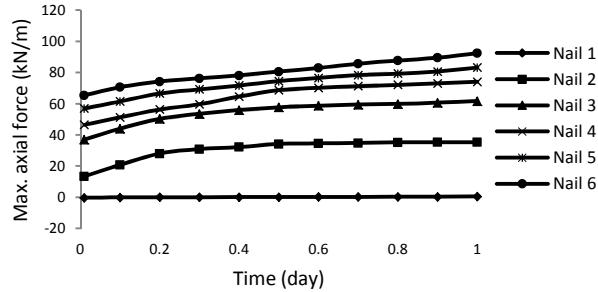
Fig. 7. Variation of axial forces for different nails at different time intervals for the slope with = 70˚a) i = 25.83 mm/hr, b) i = 20 mm/hr, and c) i = 13.75 mm/hr

On the contrary, in case of the slope with = 70˚ (**Error! Reference source not found.**), the axial forces are increasing at a higher rate compared to former case and the highest values reached for Nail 1 for rainfall intensities 25.83, 20, and 18.75 mm/hr are 112.8, 109.4, and 92.4 kN/m respectively.
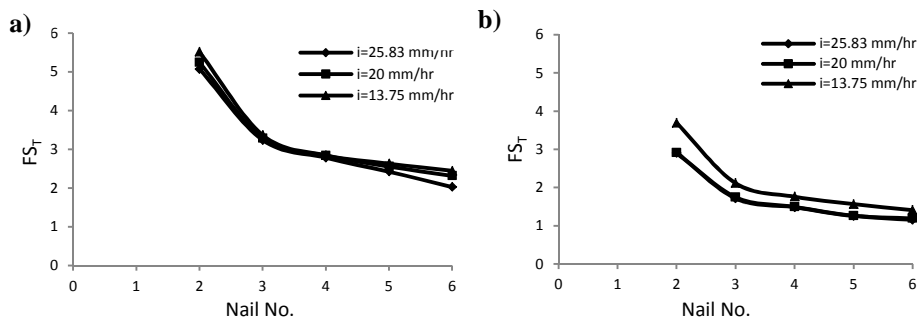
Fig. 8. Factor of safety against nail tensile strength failure (FS_T), a) = 60˚ and b) = 70˚

The relation between the factor of safety against tensile strength failure (FS_T) and nail number embedded at different depths is shown in **Error! Reference source not found.**. It is depicted from the figure that the factor of safety against tensile strength failure (FS_T) decreases with an increase in the depth of nail embedment from the top of the slope. FS_T being very high for nail 1, it is excluded from the figure. For i = 25.83 mm/hr, FS_T for bottom most nail in case of slope with = 70˚ is 1.15 and with = 60˚ is 2.02. Therefore, nails at lower portion experiences much higher forces compared to the top nails.

6   Conclusions

A series of numerical analysis was conducted under a fully coupled flow-deformation in PLAXIS finite-element modeling code. The numerical experiments to check the stability of slope were performed under two states and the conclusions that were drawn from the analysis are as follows:

- The examination results demonstrated that the deformation of the slope was large in case of steeper slope and was significantly reduced by the impact of soil nails. Consequently, a continuous slip surface was developed in case of the unreinforced slope, which may cause a shallow failure.
- After the initiation of rainfall, negative pore-water pressure starts to dissipate at the shallower depths which results in a decrease in stability. Although there was not much change in pore-water pressure profile due to the introduction of soil nails, the continuous slip surface development was prevented in the slope.
- The maximum axial forces for nails were mainly tensile in nature and for the nails selected in this study, the value was minimum for the nail in the upper portion of slope and highest for the nail in the lower portion. Also, for the steeper slope with higher rainfall intensity, the rate of increase of axial force is high compared to the other case.

References

1. Cai, F., Ugai, K.: Numerical Analysis of Rainfall Effects on Slope Stability. Int. J. Geomech. 4, 69–78 (2004). doi:10.1061/(ASCE)1532-3641(2004)4:2(69)
2. Zhang, L.L., Fredlund, D.G., Zhang, L.M., Tang, W.H.: Numerical study of soil conditions under which matric suction can be maintained. Can. Geotech. J. 41, 569–582 (2004). doi:10.1139/t04-006
3. Collins, B.D., Znidarcic, D.: Stability Analyses of Rainfall Induced Landslides. J. Geotech. Geoenvironmental Eng. 130, 362–372 (2004). doi:10.1061/(ASCE)1090-0241(2004)130:4(362)
4. Rahimi, A., Rahardjo, H., Leong, E.-C.: Effect of hydraulic properties of soil on rainfall-induced slope failure. Eng. Geol. 114, 135–143 (2010). doi:10.1016/J.ENGGEO.2010.04.010
5. Chinkulkijniwat, A., Horpibulsuk, S., Semprich, S.: Modeling of Coupled Mechanical–Hydrological Processes in Compressed-Air-Assisted Tunneling in Unconsolidated Sediments. Transp. Porous Media. 108, 105–129 (2015). doi:10.1007/s11242-014-0295-6
6. Yubonchit, S., Chinkulkijniwat, A., Horpibulsuk, S., Jothityangkoon, C., Arulrajah, A., Suddeepong, A.: Influence Factors Involving Rainfall-Induced Shallow Slope Failure: Numerical Study. Int. J. Geomech. 17, 04016158 (2017). doi:10.1061/(ASCE)GM.1943-5622.0000865
7. Luo, S.Q., Tan, S.A., Yong, K.Y.: Pull-out Resistance Mechanism of a Soil Nail Reinforcement in Dilative Soils. Soils Found. 40, 47–56 (2000). doi:10.3208/sandf.40.47
8. Yuan, J.-X., Yang, Y., Tham, L.G., Lee, P.K.K., Tsui, Y.: New Approach to Limit Equilibrium and Reliability Analysis of Soil Nailed Walls. Int. J. Geomech. 3, 145–151 (2003). doi:10.1061/(ASCE)1532-3641(2003)3:2(145)
9. Babu, G.L.S., Singh, V.P.: Reliability analysis of soil nail walls. Georisk Assess. Manag. Risk Eng. Syst. Geohazards. 3, 44–54 (2009).

doi:10.1080/17499510802541425

10. Brinkgreve, R.B.J., Swolf, W.M., Engine, E.: PLAXIS: Users manual, (2010)

11. Richards, L.A.: Capillary Conduction of Liquids through Porous Mediums. Physics (College. Park. Md). 1, 318–333 (1931). doi:10.1063/1.1745010

12. Babu, G.L.S., Singh, V.P.: Plaxis practice - Stabilization of vertical cut using soil nailing. Plaxis Bull. October, N, 6–9 (2007)

13. Dar, A.Q., Maqbool, H.: Rainfall Intensity-Duration-Frequency Relationship for different regions of Kashmir Valley (J&K) India. In: 3rd International Conference on Science and Management. pp. 651–662. , India International Centre, New Delhi (2016)

14. Dingman, S.L.: Physical hydrology. Prentice Hall, Upper Saddle River, NJ. (2002)